Journal of Solid State Chemistry **161,** 402–409 (2001)
doi:10.1006/jssc.2001.9355, available online at http://www.idealibrary.com on IDEAL®

Enthalpies of Formation of Lead Zirconate Titanate (PZT) Solid Solutions

Manisha V. Rane[1] and Alexandra Navrotsky[2]

Thermochemistry Facility, Department of Chemical Engineering and Materials Science, University of California at Davis, Davis, California 95616

and

George A. Rossetti, Jr.

Research and Development Group, Continuum Control Corporation, Billerica, Massachusetts 01821

Received May 16, 2001; in revised form August 3, 2001; accepted August 9, 2001

The formation energetics and heats of mixing of lead zirconate titanate (PZT) $PbZr_xTi_{1-x}O_3$ solid solutions have been investigated using high-temperature oxide melt solution calorimetry. While the heat content ($H_{973}-H_{298}$) is almost constant (80–82 kJ/mol) for $x = 0.15$–1.0, its value for $PbTiO_3$ ($x = 0.0$) is larger (86.15 ± 0.55 kJ/mol). Linear variation in the enthalpy of drop solution, ΔH_{ds}, and the enthalpy of formation from the oxides, $\Delta H_{f,ox}$ (298 K), is observed in the tetragonal region ($0 < x < 0.5$) and continues smoothly into part of the rhombohedral region ($0.5 < x < 0.65$). Fitting the data in the tetragonal phase region ($0 < x < 0.5$) to a straight line enables an extrapolation to give the heat of the virtual transformation $PbTiO_3$ (tetragonal → orthorhombic) as 24.0 ± 3.9 kJ/mol. An extrapolation from the rhombohedral region gives 33.3 ± 3.6 kJ/mol for ΔH of the virtual transition $PbZrO_3$ (orthorhombic or rhombohedral → tetragonal). The transition enthalpy between orthorhombic and rhombohedral $PbZrO_3$ is zero within experimental error. The enthalpy of formation from the oxides, $\Delta H_{f,ox}$(298 K), varies from -36.7 ± 2.7 kJ/mol for $PbTiO_3$ to 0.7 ± 4.3 kJ/mol for $PbZrO_3$. The $\Delta H_{f,ox}$(973 K) values agree with previously reported $\Delta H_{f,ox}$ values measured in alkali borate solvent at 1073 K. Fitting ΔH_{mix}(973 K) to a regular solution model yields an interaction parameter, W, of 39.8 ± 4.6 kJ/mol. However, structural complexity makes the regular solution model only a crude physical description. © 2001 Academic Press

Key Words: **PZT; calorimetry; enthalpy of formation; heat of mixing; enthalpy of transition.**

INTRODUCTION

Lead zirconate titanate (PZT) $PbZr_xTi_{1-x}O_3$ solid solutions are an important family of perovskites, useful for their ferroelectric and piezoelectric properties (1, 2). Electroceramics based on PZT are used extensively for electromechanical transducers, actuators, pyroelectric detectors, and explosively induced charge storage devices (3, 4). Most applications are based on the bulk ceramic form of the material, and manipulating the crystal and defect chemistry, domain configuration, and microstructure for a particular application requires an intimate understanding of the complex relations between the intrinsic and extrinsic properties (5). Studies of such structure–property relations are further complicated by difficulty in obtaining good quality single crystals and/or well-characterized polycrystalline specimens for compositions across the entire phase diagram. The two end members, $PbTiO_3$ and $PbZrO_3$, have very different structural and ferroelectric properties. Under ambient conditions, the former is a ferroelectric with tetragonal symmetry (*P*4*mm*), while the latter is an antiferroelectric with orthorhombic symmetry with a large unit cell containing 40 atoms (*Pbam*/*Pba*2). The intermediate compositions vary from tetragonal to rhombohedral (*R*3*c* or *R*3*m*) symmetry, depending upon the Zr concentration (4). A continuous cubic solid solution (*Pm*3*m*), which is of too high symmetry to exhibit ferroelectric or ferroelastic behavior, exists at high temperature, terminated at lower temperature by displacive phase transitions. This cubic solid solution, formed during high-temperature synthesis, transforms to various ferroic species on cooling. The mechanisms and kinetics of these transitions control the morphologies, microstructures, domain configurations, and properties of the ferroic species and are dictated by the thermodynamics of both the high- and low-temperature phases.

---

[1] Present address: GE Corporate Research and Development Center, Niskayuna, NY 12309.

[2] To whom correspondence should be addressed. Fax: 530-752-9307. E-mail: anavrotsky@ucdavis.edu.

0022-4596/01 $35.00

There have been some studies of phase transition enthalpies in PZT by differential thermal analysis (DTA) and differential scanning calorimetry (DSC); the DSC study by Rossetti and Navrotsky (6) is a recent example. In contrast, the formation enthalpies of PZT solid solution have not been reported. Difficulty in dissolving highly refractory oxides such as ZrO_2 and TiO_2 in aqueous solvents precludes conventional acid solution calorimetry. Recent developments in high-temperature oxide melt solution calorimetry now make it possible to measure the energetics of such refractory titanates and zirconates (7–9). The present work reports formation enthalpies and heats of mixing of PZT solid solutions. Data referring both to the high-temperature continuous cubic solid solution at 973 K and to the low-temperature partial solid solutions with lower symmetry at 298 K are discussed.

EXPERIMENTAL METHODS

Samples for calorimetric study were synthesized from chemically derived precursors of starting compositions of formula $PbZr_xTi_{1-x}O_3$ using the general procedures described in previous papers (10, 11). Prior studies (12) have shown that careful control of lead stoichiometry, precursor decomposition, calcination, and annealing are important to obtain high-quality samples suitable for calorimetric investigations. Detailed characterization by conventional and high-resolution X-ray diffraction, differential scanning calorimetry, and electron microprobe analysis (6, 10, 11) were used to ensure phase purity, crystallinity, and chemical homogeneity in the samples used in this study. The samples were stoichiometric and homogeneous within the uncertainties of microprobe analysis ($\pm$ 0.5 wt% oxides).

Thermochemical measurements were performed in a high-temperature twin Calvet calorimeter operating at 973 K using molten sodium molybdate ($3Na_2O \cdot 4MoO_4$) as solvent. The details of calorimetry have been described previously (7–9). About 20 g of sodium molybdate was equilibrated overnight in a platinum crucible in the calorimeter. Oxygen gas was bubbled through the molten molybdate solvent at 10 ml/min to stir the melt to facilitate dispersion and dissolution of the sample. The oxygen gas also maintained a well-defined high oxygen fugacity of 1 atm. A continuous flow of oxygen at 100 ml/min was also maintained above the solvent. PZT pellets weighing $\sim$ 15 mg were dropped into the solvent. The measured heat effect (ΔH_{ds}, the heat of drop solution) was the sum of the heat content from room temperature to 973 K (also known as the enthalpy of the transposed temperature drop experiment, ΔH_{ttd}), and the heat of solution at 973 K (ΔH_{sol}). At least six calorimetric experiments were performed for each composition.

The heat content (ΔH_{ttd}) was obtained by dropping $\sim$ 15-mg pellets into the calorimeter in the absence of solvent. The heat of solution (ΔH_{sol}) was measured directly for certain samples. For solution calorimetry, the sample was placed in a platinum sample holder with a perforated foil bottom and equilibrated in the calorimeter just above the solvent. The sample holder was dipped into the solvent and pulled out several times in quick succession in order to disperse and dissolve the sample. This process of stirring was repeated five times. Because the measured heat included the disturbance due to the stirring effect, a similar experiment without the sample was performed immediately afterward to determine the contribution from the stirring effect. The stirring correction generally accounted for 10 to 15% of the total observed heat effect.

Calibration of the calorimeter was based on the heat content of platinum (for solution experiments) and of corundum (for transposed temperature drop and drop solution experiments). These procedures have been discussed previously (7–9) and represent standard laboratory protocol. Calibration factors have remained content (with random fluctuations of $\pm$ 0.5%) on each side of the calorimeter for several years. The calibration is insensitive to slight variation in the glass- and platinum-ware in the calorimeter, to gas flow, and to other small variations in set-up. However, sample pellets dropped into the calorimeter pick up a small amount of heat ($<$ 1%, corresponding to an average temperature rise of $<$ 10 K) during the drop, and this is accounted for in the alumina pellet calibration. It is important to keep the mass and shape of the pellets used for calibration and for sample drop very similar.

With increasing Zr content it became progressively more difficult to obtain reproducible values for drop solution enthalpies. These Zr-rich materials dissolved slowly and showed very small heat effects because the endothermic heat content and the exothermic heat of solution nearly cancelled each other, producing a small net heat of drop solution with large relative error. The small baseline shifts, which inevitably occurred and were not significant with larger heat effects, became important in measuring small heat effects because one had difficulty telling when the reaction was complete. Thus, the values obtained became subjective. This problem could be overcome with solution calorimetry, which provided a direct measure of enthalpy of solution at 973 K for the materials with $x = 0.65$, 0.7, 0.8, 0.9, and 1.0. The enthalpies of drop solution were then calculated by adding the heat content to the heat of solution. For use in further calculations, values of the enthalpy of drop solution were calculated from the solution data for compositions $x = 0.7$ to 1.0. The rest of the ΔH_{ds} values used in calculations were taken directly from the drop solution experiments.

RESULTS AND DISCUSSION

The calorimetric data are given in Table 1. The heat of formation was obtained using suitable thermodynamic

TABLE 1
Calorimetric Data for $PbZr_xTi_{1-x}O_3$

	Measured enthalpy (kJ/mol)			Calculated enthalpy (kJ/mol)	
x	ΔH_{ttd}	ΔH_{ds}	ΔH_{sol}	$\Delta H_{ds}{}^{a}$	$\Delta H_{sol}{}^{b}$
0.00	86.15 ± 0.55 (12)[c]	74.13 ± 2.04 (8)			-12.02 ± 2.11[d]
0.15	81.38 ± 0.77 (12)	57.01 ± 1.48 (6)			-24.37 ± 1.67
0.30	80.62 ± 0.49 (6)	41.18 ± 0.67 (8)			-39.44 ± 0.83
0.40	81.30 ± 0.71 (7)	33.16 ± 0.90 (8)			-48.14 ± 1.15
0.48	81.3 ± 0.96 (7)	26.58 ± 2.20 (8)			-54.72 ± 2.40
0.50	80.1 ± 0.71 (6)	25.45 ± 2.12 (8)			-54.65 ± 2.32
0.56	80.19 ± 0.55 (8)	17.87 ± 0.72 (6)			-62.32 ± 0.90
0.65	80.92 ± 1.27 (8)	11.15 ± 2.08 (7)	$(-60.10 \pm 7.37$ (5))[e]	(20.82 ± 7.48)[e]	-69.77 ± 2.44
0.70	80.33 ± 1.02 (6)		-69.40 ± 2.26 (6)	10.93 ± 2.48	
0.80	81.26 ± 0.90 (10)	11.58 ± 1.71 (11)	-69.13 ± 1.52 (7)	12.13 ± 1.77	-69.68 ± 1.93
0.90	81.99 ± 0.89 (11)		-75.29 ± 1.93 (7)	6.70 ± 2.12	
1.00	81.49 ± 0.68 (8)	$(-10.44 \pm 2.67$ (17))[e]	-83.74 ± 3.52 (6)	-2.25 ± 3.58	(-91.93 ± 2.75)[e]

[a] $\Delta H_{ds} = \Delta H_{ttd} + \Delta H_{sol}$.
[b] $\Delta H_{sol} = \Delta H_{ds} - \Delta H_{ttd}$.
[c] The error is two standard deviations of the mean; number in parentheses is the number of experiments performed.
[d] The errors propagated for errors in both sets of measurements, i.e., error = $[(\text{error, ttd})^2 + (\text{error, sol})^2]^{0.5}$.
[e] Values in parentheses not used in further calculations.

cycles (Table 2). The additional thermodynamic data needed for the calculation of enthalpies of formation from the oxides are listed in Table 3. Solution calorimetric data for binary oxides are taken from other work in our laboratory (13, 14). For calculation of enthalpies of formation from the elements, the enthalpies of formation of binary oxides in the tabulation of Robie and Hemingway (15) were used.

Heat Contents

The variation of heat content ($\Delta H_{ttd} = H_{973} - H_{298}$) with $x = \text{Zr}/(\text{Zr} + \text{Ti})$ is shown in Fig. 1. ΔH_{ttd} remains approximately constant (80.1–82.0 kJ/mol) for $x = 0.15$ to 1.0. The heat content values calculated from the Kopp–Neumann rule (sum of appropriately weighted heat contents for PbO, ZrO_2, and TiO_2) is shown in the same plot as a straight line. All samples with $x > 0.15$ deviate from the Kopp–Neumann rule and have significantly smaller heat contents. The heat content of $PbTiO_3$ is 86.15 kJ/mol, significantly above that of a mixture of PbO and TiO_2 (14).

The heat content, ΔH_{ttd}, includes the enthalpy of phase transition from the ferroelectric to the paraelectric state. Rossetti and Navrotsky have measured the enthalpy of

TABLE 2
Thermodynamic Cycles

Heat of Formation of $PbZr_xTi_{1-x}O_3$ from Oxides at 298 K	
PbO (cr., 298 K) = PbO (dil. sol., 973 K)	ΔH_{ds}(PbO)
$(x)ZrO_2$ (cr., 298 K) = $(x)ZrO_2$ (dil. sol., 973 K)	$(x)\Delta H_{ds}(ZrO_2)$
$(1-x)TiO_2$(cr., 298 K) = $(1-x)TiO_2$(dil. sol., 973 K)	$(1-x)\Delta H_{ds}(TiO_2)$
$PbZr_xTi_{1-x}O_3$ (cr., 298 K) = $[PbO + (x)ZrO_2 + (1-x)TiO_2]$ (dil. sol., 973 K)	$\Delta H_{ds}(PbZr_xTi_{1-x}O_3)$

$PbO + (x)ZrO_2 + (1-x)TiO_2 = PbZr_xTi_{1-x}O_3$

$\Delta H_{f,ox}(PbZr_xTi_{1-x}O_3)(298\text{ K}) = \Delta H_{ds}(PbO) + (x)\Delta H_{ds}(ZrO_2) + (1-x)\Delta H_{ds}(TiO_2) - \Delta H_{ds}(PbZr_xTi_{1-x}O_3)$

$\Delta H_{f,ox}(PbZr_xTi_{1-x}O_3)(973\text{ K}) = \Delta H_{sol}(PbO) + (x)\Delta H_{sol}(ZrO_2) + (1-x)\Delta H_{sol}(TiO_2) - \Delta H_{sol}(PbZr_xTi_{1-x}O_3)$

Heat of Formation of $PbZr_xTi_{1-x}O_3$ from Elements in Standard States at 298 K	
$PbO + (x)ZrO_2 + (1-x)TiO_2 = PbZr_xTi_{1-x}O_3$	$\Delta H_{f,ox}(PbZr_xTi_{1-x}O_3)$ (298 K)
$Pb + (1/2)O_2 = PbO$	$\Delta H^0_{f,el}$(PbO) (298 K)
$(x)Zr + (x)O_2 = ZrO_2$	$(x)\Delta H^0_{f,el}(ZrO_2)$ (298 K)
$(1-x)Ti + (1-x)O_2 = TiO_2$	$(1-x)\Delta H^0_{f,el}(TiO_2)$ (298 K)

$Pb + (x)Zr + (1-x)Ti + (1.5) = O_2 = PbZr_xTi_{1-x}O_3$

$\Delta H^0_{f,el}(PbZr_xTi_{1-x}O_3) = \Delta H_{f,ox}(PbZr_xTi_{1-x}O_3) + \Delta H^0_{f,el}(PbO) + (x)\Delta H^0_{f,el}(ZrO_2) + (1-x)\Delta H^0_{f,el}(TiO_2)$

TABLE 3
Additional Thermochemical Data Used to Calculate Enthalpies of Formation of $PbZr_xTi_{1-x}O_3$ from the Oxides

	Enthalpy (kJ/mol)	
Compound	ΔH_{ttd}	ΔH_{ds}[a]
PbO (litharge)	37.2[b]	– 21.5 ± 1.5[c]
ZrO_2 (baddeleyite)	47.3[b]	19.7 ± 1.8[d]
TiO_2 (rutile)	44.2[b]	58.9 ± 0.8[d]

[a] Solvent is $3Na_2O \cdot HMoO_3$ at 973 K.
[b] Literature values of heat content (15, 21).
[c] Measured, this study, from thermochemical cycle using $PbCO_3$.
[d] Measured, this laboratory (13, 14).

phase transition by DSC to be 1.93 ± 0.05, 0.96 ± 0.05, 0.39 ± 0.05, and 0.00 ± 0.05 kJ/mol for $x = 0$, 0.15, 0.3, and 0.4, respectively (6). These small enthalpies of transition would contribute increments to the heat content which are smaller than the variation of about 2 kJ/mol seen in ΔH_{ttd} for $x = 0.15$ to 1.0. Thus, ΔH_{ttd} is observed to be nearly constant for $x = 0.15$ to 1.0, despite the presence of structural phase transitions.

The positive deviation from the Kopp–Neumann rule for $PbTiO_3$ contrasts with the negative deviation at other, more Zr-rich, compositions. The Kopp–Neumann additivity rule is not expected to hold very well for PZT because the coordination and local bonding of cations in the perovskite differ from those in the binary oxides. For Ti-rich compositions, one can compare the octahedral environment of Ti in rutile and in the perovskite B-site. The latter octahedra are not edge shared and are free to rotate (causing the deviation from cubic symmetry at low temperature). Thus, a higher heat capacity in the perovskite seems reasonable. In Zr-rich compositions, the 7-fold distorted coordination of Zr in baddeleyite contrasts with the regular 6-fold coordination in the perovskite B-site. The latter represents tighter bonding with a shorter Zr–O bond length, thus rationalizing its lower average heat capacity.

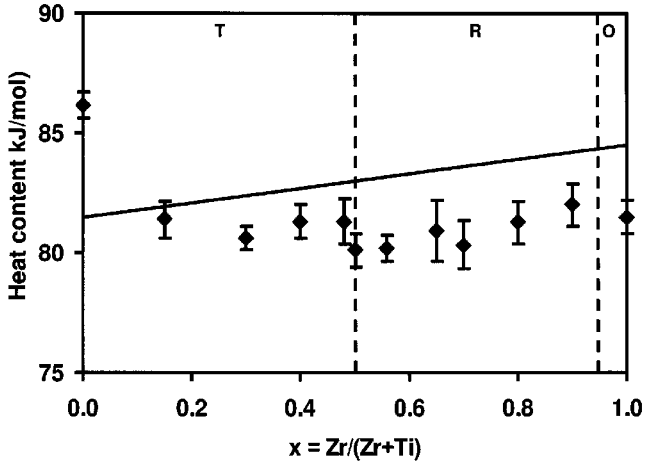

FIG. 1. Heat content ($H_{973} - H_{298}$) versus $x = Zr/(Zr + Ti)$.

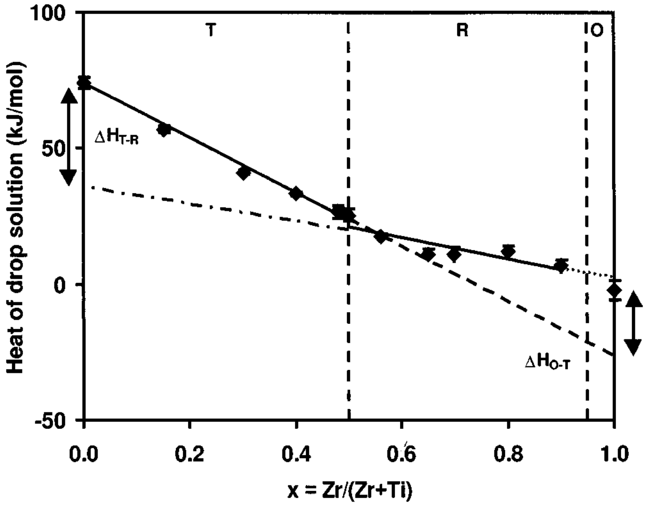

FIG. 2. Heat of drop solution in $3Na_2O \cdot 4MoO_4$ at 973 K versus $x = Zr/(Zr + Ti)$.

Heats of Drop Solution and Enthalpy Differences between Different Structures at 298 K

Figure 2 shows the variation of the heat of drop solution, ΔH_{ds}, with composition. The three different regions, tetragonal (T, $x = 0$ to 0.5), rhombohedral (R, $x = 0.5$ to 0.95), and orthorhombic (O, $x = 0.95$ to 1.0), are demarcated by dashed lines. ΔH_{ds} decreases with increasing x from 74.13 ± 2.04 kJ/mol for $PbTiO_3$ to – 2.25 ± 3.58 kJ/mol for $PbZrO_3$.

Because $\Delta H_{ds} = \Delta H_{ttd} + \Delta H_{sol}$, simultaneous measurement of all three enthalpies (by drop solution, transposed temperature drop, and solution techniques, respectively, as described above) allows a check of internal consistency of the data. Despite the small heat effects and proportionately large baseline corrections encountered in the drop solution experiments, consistency is observed between the directly measured enthalpy of drop solution and the sum of heat content and heat of solution for $x = 0.8$, namely 11.58 ± 1.71 kJ/mol and 12.13 ± 1.77 kJ/mol, respectively. The consistency suggests that the scatter in the data does not introduce any systematic bias in either set of measurements. For $x = 1.0$, the ΔH_{ds} calculated from the solution experiments is more endothermic (– 2.25 ± 3.58 kJ/mol) than that obtained from drop solution experiments (– 10.44 ± 2.67 kJ/mol). For $x = 0.65$, a value of 11.15 ± 2.08 kJ/mol is obtained from drop solution experiments and 20.82 ± 7.48 kJ/mol from solution experiments.

The differences, at or slightly beyond the range of the statistical uncertainties, reflect the sluggish dissolution and small heat effects associated with these Zr-rich samples.

Some observations related to the particle size distribution of the samples may be relevant to the discrepancies seen in solution and drop solution calorimetric data for samples with high Zr content. Depending on composition the average particle size ranged from ~ 5 μm to ~ 50 μm. It is likely that these larger grains contributed to the slower dissolution of samples with $x = 0.65$ and 1.0. The larger scatter in the calorimetric data and the larger baseline drifts may be related to somewhat variable grain size distribution in different calorimetric runs, and slow dissolution or local saturation of the solvent in the vicinity of the larger grains. The relatively larger scatter in data from solution calorimetry might also be due to further coarsening during equilibration of the sample for 8–12 hrs at 973 K before starting the experiment. We note that the grain size is difficult to control because different calcination temperatures are needed for different zirconium contents. Other differences in morphology and microstructure may also affect dissolution rates.

The ΔH_{ds} data in the tetragonal region, $x = 0$ to 0.5, were fitted to a straight line, which can be extrapolated into the orthorhombic phase region. From the extrapolated value $x = 1.0$, the enthalpy of the hypothetical transformation of $PbTiO_3$ from tetragonal to orthorhombic, $\Delta H_{\mathrm{T\text{-}O}}$, was calculated to be 24.6 ± 3.9 kJ/mol. Similarly, the heat of the hypothetical transformation of $PbZrO_3$ from rhombohedral to tetragonal, $\Delta H_{\mathrm{R\text{-}T}}$, was calculated to be 33.3 ± 4.1 kJ/mol. The heat of the virtual transformation for $PbZrO_3$ from rhombohedral to orthorhombic, $\Delta H_{\mathrm{O\text{-}R}}$, appears to be very small and can be taken to be zero within experimental error (± 2 kJ/mol). Thus, the enthalpy of the virtual transformation of $PbZrO_3$ from orthorhombic to tetragonal, $\Delta H_{\mathrm{O\text{-}T}}$, can be taken as equal to $\Delta H_{\mathrm{R\text{-}T}}$. We call these transformations virtual because the phases $PbTiO_3$ (orthorhombic), $PbZrO_3$ (tetragonal), and $PbZrO_3$ (rhombohedral) do not exist (they are sometimes called cryptomodifications). Nevertheless, their energies relative to those of the stable polymorphs are of interest from the point of view of systematics.

Heats of Solution and Enthalpies of Mixing in the Cubic Solid Solution at 973 K

Figure 3 shows the variation of ΔH_{sol} with x. The ΔH_{sol} (973 K) values refer to the cubic form rather than the room-temperature structures. The data for $x = 0$ to 0.65 were obtained by subtracting the heat content from the drop solution enthalpies. The rest were obtained directly from the solution-experiments. The data were analyzed in this way to take advantage of the more accurate measurements at each composition. ΔH_{sol}(973 K) varies from -12.02 ± 2.11 kJ/mol for $PbTiO_3$ to -83.74 ± 3.52 kJ/mol for $PbZrO_3$. The straight line joining the two end members denotes the ΔH_{sol} of a mechanical mixture or an ideal solid solution. Most of the data show a negative deviation from this straight line, implying a positive heat of mixing. The ΔH_{sol}(973 K) data were fitted to a regular solution model:

$$\Delta H_{\mathrm{sol}} = x\Delta H_{\mathrm{sol}}(\mathrm{PbZrO_3}) + (1-x)\Delta H_{\mathrm{sol}}(\mathrm{PbTiO_3}) - Wx(1-x).$$

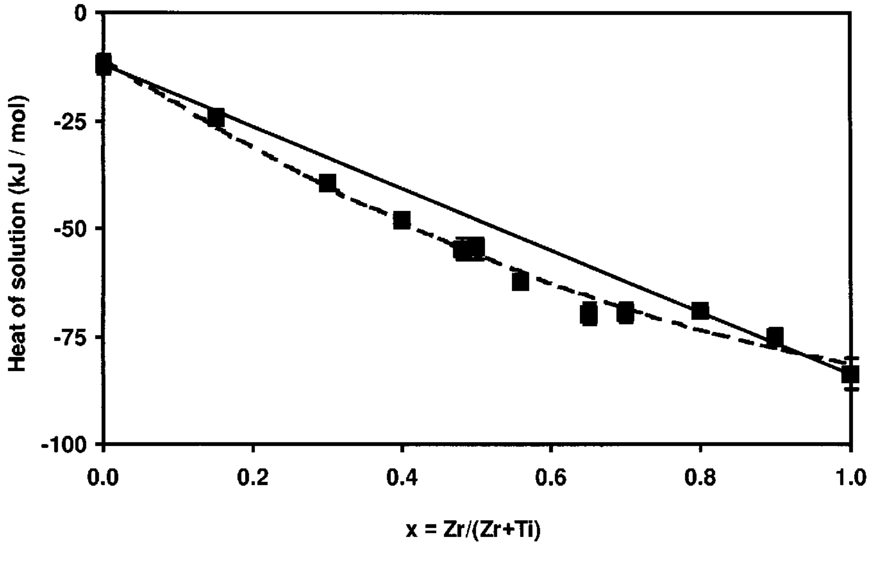

FIG. 3. Heat of solution in $3Na_2O \cdot 4MoO_4$ at 973 K versus $x = \mathrm{Zr/(Zr + Ti)}$.

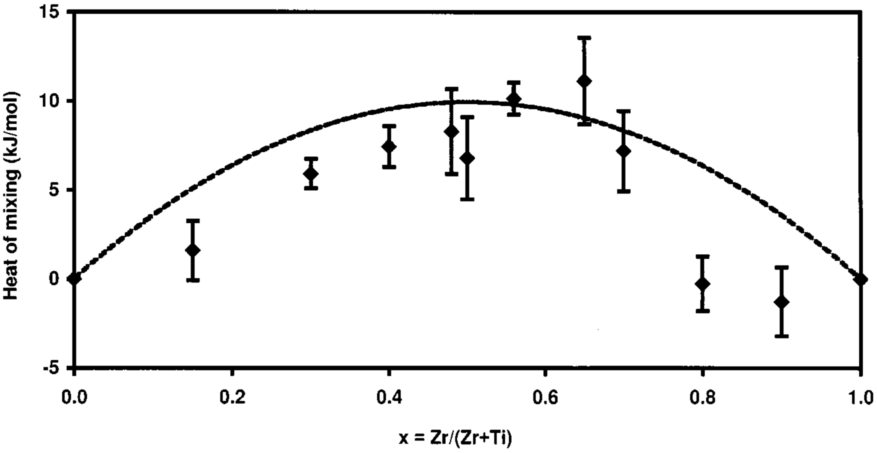

FIG. 4. Heat of mixing at 973 K versus $x = \mathrm{Zr}/(\mathrm{Zr} + \mathrm{Ti})$. The curve is calculated for a regular solution with $W = 39.8$ kJ/mol. The points are calculated from the heats of solution.

The value for the interaction parameter, W, is 39.8 ± 4.7 kJ/mol. The calculated heats of mixing in the cubic phase at 973 K,

$$\Delta H_{\mathrm{mix}} = Wx(1 - x) = (39.8 \pm 4.7)x(1 - x),$$

are compared with experimental values in Fig. 4. The uncertainties in the heats of mixing are propagated from the errors in heats of solution. In addition, there may be small systematic errors, primarily related to variations in sample composition and homogeneity. The total uncertainty is probably about 1.5 times the statistical error. The regular solution model describes the data to a useful first approximation, but, since the actual behavior in the cubic phase is almost certainly more complex, this model should not be taken to have physical significance.

Another indication of such structural and thermodynamic complexity is given by the following argument. If the regular solution approximation were rigorously valid, a symmetrical solvus would appear with a critical temperature of $W/2R$ or about 2400 K. This does not appear to be the case, since cubic solid solutions without obvious unmixing can be synthesized and persist down to temperatures below 1000 K where phase transitions to structures of lower macroscopic symmetry are seen. It is conceivable that the cubic solid solution is stabilized by a significant positive excess vibrational entropy, but there is no direct evidence for this, either in the measured heat contents or in other thermodynamic data. It is also possible that the observed cubic phase is metastable. Furthermore, the detection of incipient unmixing (compositional variation at the nanoscale and/or lowering of the symmetry from cubic in nanodomains) is very difficult to detect, especially by normal laboratory-based X-ray diffraction at the high temperature needed to study the nonquenchable cubic solid solution. Thus, there may be greater structural complexity on the scale of individual unit cells or bond lengths. It has been proposed that in cubic PZT there are two sets of B-site bond lengths, shorter Ti–O bonds and longer Zr–O bonds, with a difference of ~4.5% (16). The Pb–O bond lengths differ by 2.5% from predictions based on ionic radii. The ferroelectric state enhances the Ti–O hybridization, leading to formation of very short covalent Ti–O bonds, while the other Ti–O bonds are broken. Pb–O hybridization leads to covalent chain formation with very short Pb–O bonds. Neither breaking of Zr–O bonds nor formation of any stronger covalent Zr–O bonds takes place with Ti substitution (16). In the diffusionless structural phase transition to the cubic phase, the deformation of unit cells along the polar direction in the ferroelectric region becomes zero in the paraelectric region. However, individual polyhedra and unit cells may still be distorted, but not aligned. Thus, the cubic phase probably contains strain, local heterogeneity, and distortions and tilts at the level of individual polyhedra. These may well persist to several hundred degrees above the transition temperature. Such distortions may reflect lattice relaxation involving cation shifts and/or octahedral tilts, premonitory optic mode softening, order–disorder behavior, variation in bond lengths, changes in bond hybridization and the lone pair effect, or combinations thereof. Thus, the structural, crystal chemical, and lattice dynamical features of the prototypic cubic phase are likely very complex and are responsible for the diversity of displacive transitions into the ferroic symmetries. Description of the thermodynamics of these complex phenomena in the high-temperature phase by the simple regular solution formalism may not be physically meaningful.

ΔH_{sol} is a measure of the energy required for breaking the bonds in the crystalline compound to produce dissolved ionic species at dilute concentrations in the molten oxide solvent (16). ΔH_{sol}(973 K) varies from -12.02 ± 2.11 kJ/mol for $PbTiO_3$ to -83.74 ± 3.52 kJ/mol for $PbZrO_3$. This means that more energy is released when the sample dissolves as Zr is substituted for Ti, which is consistent with a decrease in bond strength or lattice energy as the larger Zr^{4+} ion is substituted for the smaller Ti^{4+} ion in PZT. ΔH_{sol} of TiO_2 is 14.69 ± 0.82 kJ/mol, while that of ZrO_2 is -27.6 ± 1.80 kJ/mol (see Table 3). Thus, the ΔH_{sol} of the mixture of the individual oxide components follows a similar pattern as ΔH_{sol} of PZT, namely a trend toward more exothermic values with increasing Zr content, but with a slope which is only about half of that for PZT. This indicates that PZT becomes progressively less stable with respect to its component oxides with increasing Zr content; see below. This sequence of stability is also seen in an equilibrium isothermal section measured at 1100°C (4) and in the phase formation sequence on reaction of the component oxides, where Ti-rich phases form first (12). The common observation that when lead is lost at high temperature, the Ti-rich phases become stable (4) also supports this thermodynamic trend.

Enthalpies of Formation

The enthalpy of formation from the oxides, $\Delta H_{f,ox}$(298 K), and $\Delta H_{f,ox}$ (973 K), is shown in Table 4. Takayama-Muromachi and Navrotsky (18) reported $\Delta H_{f,ox}$(1068 K) from solution calorimetry in alkali borate for the two end members $PbTiO_3$ and $PbZrO_3$ as -31.1 ± 4.1 kJ/mol and 1.7 ± 6.6 kJ/mol, respectively. Their values, though measured in a different solvent and at a temperature 100 K higher than in the present study, agree with our values of -32.06 ± 2.70 kJ/mol and -2.63 ± 4.22 kJ/mol, respectively. Consistency among data obtained in two different solvents is an additional indication of trouble-free calorimetry. The calorimetric value for $PbTiO_3$ agrees very well with an enthalpy of formation of -32.51 ± 2.25 kJ/mol obtained from the temperature dependence of solid cell electrochemical measurements at 1090–1350 K (19). A similar electrochemical study of $PbZrO_3$ at 800–1400 K (20) gives $\Delta H_{f,ox} = -4.54$ kJ/mol, with the uncertainty not quoted, again in agreement with our measurements. The enthalpies of formation from the oxides for intermediate compositions, measured for the first time in this study, reflect the structural changes and mixing energetics described above. There is a clear trend of diminishing stability relative to the oxides as Zr is substituted for Ti throughout the series. Enthalpies of formation from the elements, on the other hand, become more exothermic as Zr is substituted for Ti. This simply reflects the more negative enthalpy of formation of ZrO_2 compared to that of TiO_2.

TABLE 4
Enthalpies of Formation from Oxides at 298 K and 973 K, and from Elements at 298 K

$x = Zr/(Zr + Ti)$	$\Delta H^0_{f,ox}$ (298 K)	$\Delta H^0_{f,ox}$ (973 K)	$\Delta H^0_{f,el}$(298 K)
0.0	-36.74 ± 2.65^a	-32.06 ± 2.70^a	-1199.74 ± 2.88^a
0.15	-25.50 ± 2.22^a	-26.05 ± 2.35^a	-1211.99 ± 2.56^a
0.30	-15.56 ± 1.87^a	-17.33 ± 1.87^a	-1225.54 ± 2.28^a
0.40	-11.46 ± 1.94^a	-12.86 ± 2.07^a	-1237.10 ± 2.44^a
0.48	-8.02 ± 2.82^a	-9.66 ± 2.98^a	-1246.19 ± 3.21^a
0.50	-7.67 ± 2.77^a	-10.58 ± 2.92^a	-1248.97 ± 3.17^a
0.56	-2.44 ± 1.96^a	-5.44 ± 2.04^a	-1253.14 ± 2.53^a
0.65	0.75 ± 2.82^a	-1.80 ± 3.10^a	-1264.04 ± 3.27^a
0.65	-8.92 ± 7.12^b	-11.47 ± 7.61^b	-1273.71 ± 7.87^b
0.70	-0.99 ± 3.16^b	-4.28 ± 2.99^b	-1273.61 ± 3.58^b
0.80	-5.57 ± 2.69^a	-8.23 ± 2.83^a	-1293.85 ± 3.21^a
0.80	-6.12 ± 2.72^b	-8.78 ± 2.57^b	-1294.40 ± 3.24^b
0.90	-4.61 ± 3.05^b	-6.85 ± 2.92^b	-1308.55 ± 3.55^b
1.0	8.61 ± 3.54^a	5.56 ± 3.60^a	-1310.99 ± 4.01^a
1.0	0.42 ± 4.28^b	-2.63 ± 4.22^b	-1319.18 ± 4.66^b

[a] From drop solution experiments.
[b] From solution experiments.

CONCLUSIONS

High-temperature oxide melt solution calorimetry has successfully constrained the enthalpies of formation, of mixing in the cubic phase, and of phase transformations among tetragonal, orthorhombic, and rhombohedral structures in the PZT system. Further studies are needed to correlate these bulk thermodynamic parameters to details of structure and bonding and their relation to the mechanisms of phase transition to the lower temperature symmetry-allowed ferroic phases.

ACKNOWLEDGMENTS

This work was supported by the Center for High Pressure Research, an NSF Science and Technology Center. We thank K. B. Helean, J. Majzlan, I. Molodetsky, and M. R. Ranade for calorimetric measurements on the binary oxides.

REFERENCES

1. S. Hoon Oh and H. M. Jang, *J. Appl. Phys.* **85,** 2815 (1999).
2. S. Kojima, N. Ohta, and X. Dong, *Jpn. J. Appl. Phys.* **38,** 5674 (1999).
3. Y. Xu, "Ferroelectric Materials and Their Applications." North-Holland, Amsterdam, 1991.
4. B. Jaffe, W. R. Cook, Jr., and H. Jaffe, "Piezoelectric Ceramics." Academic Press, London, 1971.
5. M. J. Haun, E. Furman, S. J. Jang, and L. E. Cross, *Ferroelectrics* **99,** 13 (1989).
6. G. A. Rossetti, Jr., and A. Navrotsky, *J. Solid State Chem.* **144,** 188 (1999).
7. A. Navrotsky, *Phys. Chem. Miner.* **24,** 222 (1997).
8. A. Navrotsky, *J. Thermal Anal. Calorim.* **57,** 653 (1999).
9. J. McHale, G. R. Kovach, A. Navrotsky, and F. DiSalvo, *Chem. Eur. J.* **2,** 1514 (1996).
10. G. A. Rossetti, Jr., L. E. Cross, and J. P. Cline, *J. Mater. Sci.* **30,** 24 (1995).

11. G. A. Rossetti, Jr., J. P. Cline, and A. Navrotsky, *J. Mater. Res.* **13,** 3197 (1998).
12. G. A. Rossetti, Jr., P. F. Cahill, Jr., R. R. Biederman, and A. Sacco, Jr., *Mater. Lett.* **41,** 72 (1999).
13. I. Molodetsky, A. Navrotsky, F. DiSalvo, and M. Lerch, *J. Mater. Res.* **15,** 2558 (2000).
14. K. B. Helean, T. Lee, I. Molodetsky, and A. Navrotsky, in preparation.
15. R. A. Robie and B. S. Hemingway, "Thermodynamic Properties of Minerals and Related Substances at 298.15 K and 1 Bar (10^5 Pascals) Pressure and at Higher Temperatures." Geological Survey Bulletin No. 2131. 1995. U.S. Government Printing Office, Washington, DC, 1995.
16. L. Bellaiche, J. Padilla, and D. Vanderbilt, *in* "AIP Conference Proceedings 436, First-Principles Calculations for Ferroelectrics, Fifth Williamsburg Workshop" (R. E. Cohen Ed.), p. 11. Carnegie Institution of Washington, Washington, DC, 1998.
17. A. Navrotsky, *Am. Mineral.* **79,** 589 (1994).
18. E. Takayama-Muromachi and A. Navrotsky, *J. Solid State Chem.* **72,** 244 (1988).
19. W. W. Shim and K. T. Jacob, *Can. Met. Quart.* **21,** 171 (1982).
20. K. T. Jacob and W. W. Shim, *J. Am. Ceram. Soc.* **64,** 573 (1981).
21. E. Barin and O. Knacke, "Thermochemical Properties of Inorganic Substances." Springer-Verlag, Berlin, 1973.